MODELLING THE DYNAMICS OF A RIGID ROTOR IN ACTIVE MAGNETIC BEARINGS

Gennadii Martynenko

Faculty of Engineering Physics, Department of Dynamics and Strength of Machines

National Technical University *Kharkiv Polytechnic Institute*

Ukraine

gmartynenko@kpi.kharkov.ua

Abstract

The paper deals with developing a mathematical model of a rigid rotor in active radial and axial electromagnetic bearings.

A feature of the suggested technique of mathematical description of rotor dynamic behaviour is accounting for the nonlinear relationship of mechanical and electromagnetic processes in the system. The magnetic conductance of gaps under the poles of the electromagnets is defined with account of the mutual impact of radial and axial rotor displacement.

The analytical model described can be used as a basis of the simulation computer model for alternative dynamic stability calculations to select effective suspension parameters and control actions for different design options.

Key words

Dynamics of rotor systems, active magnetic bearings, mathematical model

1 Introduction

Active magnetic bearings (AMB) are an alternative to frictionless, sliding and gas-dynamic bearings, and, as compared to these, have several advantages (no lubrication systems, reduced friction loss, comparatively big gap, and others) [Siegwart, Bleuler and Traxler, 2000].

During a mathematical description of a rotor-AMB system, the following parts are distinguished: the rotor mathematical model, the bearing model and the control law effected by the control system [Steven, Nataraj, 2007].

Correct definition and validation of control algorithm parameters with numerical experiments is possible only with adequate mathematical modelling of the rotor-AMB system and interrelated magnetic and mechanical phenomena occuring therein.

In analysing several technical devices, the electromechanical vibration equations are linearised. Such an approach was also used for AMB [Schweitzer, Bleuler and Traxler, 1994]. Thus, the magneto-mechanical rotor in AMB system is modelled with motion differential equations and differential equations for currents in the linear approximation. In so doing, the currents in the circuits and the control voltages in the windings are linearised about the equilibrium position [Maslen, 2000].

The suspension linear model is written down on the assumption of smallness of deviations of variables from their rated values. Actually, these deviations can be significant. Hence, in limit conditions – magnetic circuit saturation, zero current, zero gap, and so forth – the linear suspension model becomes meaningless [Zhuravlyov, 2003]. Thus, with circuit currents close to zero, linearisation about the equilibrium position is incorrect. When rotor displacements are comparable with the rated gap, the mathematical model is also incorrect.

These deficiencies can also be inherent to rotor position control units built around such linearised models.

This paper considers a nonlinear mathematical model of a rigid rotor in AMB. The model accounts for the relation between axial and radial rotor displacements when defining the magnetic conductances of gaps under the poles of magnetic bearings. The fluxes in the AMB magnetic circuits have been defined using detail equivalent circuits with account of magnetic resistances of air gaps under the poles and between them, as well as in stator and rotor sections.

In the paper, one of the possible designs of a complete electromagnetic rotor suspension with two 8-pole radial bearings and one axial bearing with an armature in the form of a pot core has been modelled.

2 Description of electromechanical systems

Technical electromechanical systems are described by Lagrange-Maxwell equations structured as mechanics equations. When conductance currents are closed and there are no capacitors in the electric paths, electromechanical systems are described by equations similar to Routh equations in mechanics

[Hodzhaev, 1979]:

$$\left.\begin{array}{l} \frac{\partial}{\partial t}\frac{\partial T}{\partial q_r} - \frac{\partial T}{\partial q_r} + \frac{\partial \Pi}{\partial q_r} = -\frac{\partial W}{\partial q_r} + Q_r \quad (r=1,...,M) \\ \frac{\partial \Psi_k}{\partial t} + \sum_{s=1}^{N} r_{Cks}\frac{\partial W}{\partial \Psi_s} = E_k \qquad (k=1,...,N) \end{array}\right\} \quad (1)$$

where T is kinetic energy; Π is potential energy; $W=W(\Psi_1,..., \Psi_N, q_1,..., q_M)$ is magnetic field energy; q_r are generalised mechanical coordinates; Q_r are nonpotential generalised forces; M is the number of generalised mechanical coordinates; Ψ_k are induction fluxes (flux linkages); N is the number of closed nonbranching loops with loop currents i_k; r_{Cks} are active resistances of electric circuits, and E_k is algebraic sum of external electromotive forces in the k-th loop, and

$$\Psi_k = \frac{\partial W}{\partial i_k}, \; i_s = \frac{\partial W}{\partial \Psi_s} \,. \qquad (2)$$

3   Rotor magnetic suspension layout

In the paper, the technique of mathematical description of the rotor-AMB system is considered by example of one of the possible alternatives of the model of the complete electromagnetic rotor suspension shown in Figure 1.
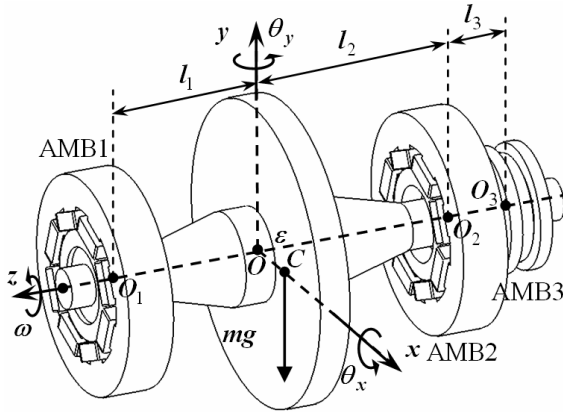

Figure 1. Model and layout of a complete electromagnetic rotor suspension.

Typical 8-pole magnetic bearings are used as two radial ones (Fig. 2), and a typical thrust magnetic bearing with pot cores is used as the axial one (Fig. 3) [Maslen, 2000].
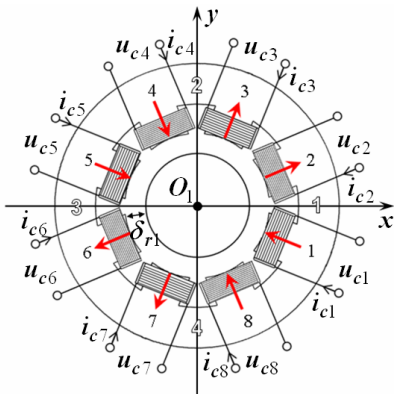

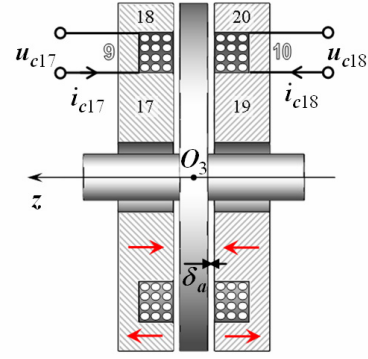Figure 2. Radial magnetic bearing AMB1.

Figure 3. Axial thrust magnetic bearing AMB3.

In Figs. 2 and 3, figures 1 to 20 denote pole numbers, and 1 to 10 denote electromagnets. Pairwise connection of pole coils in each radial bearing AMB1 and AMB2 can make four electromagnets for each bearing [Steven, Nataraj, 2007].

Control voltage u_{ck} is assumed to be applied to each pole coil. Its magnitude is defined by the control algorithm depending on the control parameters [Maslen, 2000].

The current i_{ck} in the winding of the k-th pole coil with w_k turns and ohmic resistance r_{ck} induces a magnetomotive force (MMF) $e_k=w_k i_{ck}$, which causes a magnetic flux in the AMB magnetic circuit. The directions of the fluxes in Figs. 2 and 3 are designated with red arrows.

In the rotor central position, the rated air gap between the poles of radial AMB and the journals is equal to δ_{r1} in AMB1 and δ_{r2} in AMB2 (Fig. 2). The rated air gap between the stator and the disk of the axial bearing AMB3 on each side is equal to δ_a.

4   The mathematical model of a rigid rotor

Let us consider a spatial design scheme of a rotating absolutely rigid rotor in a magnetic suspension (Fig. 1). Fixed right-hand Cartesian coordinates are introduced for uniquely positioning the rotor in space. Its origin O^* is located on the geometric longitudinal axis of the rotor, which is in the central position. The coordinate axes are associated with the rotor in this position as follows: axis O^*z coincides with the geometric longitudinal axis of the rotor, and axes O^*x and O^*y are located in a plane perpendicular to axis O^*z and pass through the centre of gravity of rotor C. For the rotor in an arbitrary position, $O(x_0,y_0,z_0)$ denotes the geometric centre of the transverse section passing through the centre of gravity of the rotor. The centres of the bearing sections of the rotor in AMB1 and AMB2 are denoted as $O_1(x_1,y_1,z_1)$ and $O_2(x_2,y_2,z_2)$ (Fig. 1). The distance between O and O_1 is equal to l_1, and that between O and O_2 is equal to l_2.

Two associated groups of generalized coordinates $\zeta=(x_0,y_0,z_0,\theta_x,\theta_y)$ or $q=(x_1,y_1,x_2,y_2,z_3)$ are used for defining the rotor position. Here, θ_x, θ_y are the angles of rotation about axes O^*x and O^*y, and z_3 is the coordinate of the centre O_3 of the AMB3 disk.

The mechanical part of the mathematical model of a rotating absolutely rigid rotor in AMB, with the number of generalized mechanical coordinates $M=5$ according to (1), is described by a system of differential equations [Poznjak, 1980]:

$$
\left.
\begin{aligned}
&m\frac{d^2 x_0}{dt^2} = Q_x - \frac{\partial W}{\partial x_0} + m\omega^2(\varepsilon_1 \cos\omega t - \varepsilon_2 \sin\omega t);\\
&m\frac{d^2 y_0}{dt^2} = Q_y - \frac{\partial W}{\partial y_0} + m\omega^2(\varepsilon_1 \sin\omega t + \varepsilon_2 \cos\omega t);\\
&m\frac{d^2 z_0}{dt^2} = Q_z - \frac{\partial W}{\partial z_0};\\
&J_e \frac{d^2 \theta_x}{dt^2} + J_p\omega\frac{d\theta_y}{dt} = Q_{\theta x} - \frac{\partial W}{\partial \theta_x} +\\
&+ (J_e - J_p)\omega^2(\gamma_1 \cos\omega t - \gamma_2 \sin\omega t);\\
&J_e \frac{d^2 \theta_y}{dt^2} - J_p\omega\frac{d\theta_x}{dt} = Q_{\theta y} - \frac{\partial W}{\partial \theta_y} +\\
&+ (J_e - J_p)\omega^2(\gamma_1 \sin\omega t + \gamma_2 \cos\omega t).
\end{aligned}
\right\} \quad (3)
$$

where m is rotor mass; e_1, e_2 and γ_1, γ_2 are linear and angular nonequilibrium parameters; J_e, J_p are rotor equatorial and polar moments of inertia; ω is angular velocity; $P_{\xi r} = -\partial W/\partial \xi_r$ are suspension electromagnetic responses, and Q are generalized external forces and moments.

5 Model of magnetic bearings

To consider the option of a complete electromagnetic suspension (Fig. 1), an AMB contains $N=18$ electromagnetic circuits with currents i_{ck}, ohmic resistances r_{ck} and input voltages u_{ck} (control signals). Saturation and magnetic hysteresis is ignored. Then the electromagnetic part of the mathematical model according to (1) includes $N=18$ differential equations with respect to flux linkages. These equations correspond to Kirchhoff's second law for magnetic circuits and are a form of notation of the net current law for each k-th circuit:

$$\frac{\partial \Psi_{ck}}{\partial t} + r_{ck}\frac{\partial W}{\partial \Psi_{ck}} = u_{ck} \quad (k = 1,...,N), \qquad (4)$$

where Ψ_{ck} is flux linkage (net magnetic fluxes through the coil circuits).

If we assume that the magnetic flux conducted by each coil turn is the same, then the total or net magnetic flux through the coil loop will be

$$\Psi_{ck} = w_k \Phi_k. \qquad (5)$$

The magnetic flux Φ_k through area S_k of a magnetic circuit section is equal to [Bessonov, 1973]

$$\Phi_k = B_k S_k. \qquad (6)$$

The magnetic resistance of a magnetic circuit section [Bessonov, 1973] is

$$R_k = \frac{l_k}{\mu_0 \mu_k S_k}, \qquad (7)$$

where l_k is length of a magnetic circuit section; S_k is cross-section area; μ_0 is permeability of vacuum; μ_k is relative magnetic permeability of the circuit section material.

Then the energy of the magnetic field of the circuit section [Bessonov, 1973] is equal to

$$W_k = \tfrac{1}{2} R_k \Phi_k^2, \qquad (8)$$

and the energy of the entire magnetic circuit is equal to the sum of energies of this circuit sections.

If W_I, W_{II} and W_{III} denote the energy of AMB1, AMB2 and AMB3 circuits, respectively, then the energy of the magnetic field in the magnetic circuits of a complete electromagnetic rotor suspension in AMB is equal to:

$$W = W_I + W_{II} + W_{III}. \qquad (9)$$

5.1 Determining magnetic fluxes

The net flux linkage of the k-th loop Ψ_{ck} is a function of both the current in the k-th loop and the currents in other loops magnetically linked with the k-th loop [Bessonov, 1973]. In this case, detail equivalent circuits are suggested to be used for correct determination of magnetic fluxes in magnetic circuit sections.

The magnetic fluxes in the magnetic circuit of the radial AMB1 are found by considering its equivalent circuit, Fig. 4.

The following designations are used in Fig. 4: Φ_k are magnetic fluxes in circuit sections, where Φ_1 to Φ_8 refer to pole sections, Φ_9 to Φ_{16} refer to air gaps under the poles, and Φ_{17} to Φ_{24} refer to stator armature; Φ_{25} to Φ_{32} are leakages through air gaps between the stator poles, Φ_{33} to Φ_{40} are leakages through the journal in the rotor, and Φ_{C1} to Φ_{C16} are loop leakages; R_k are magnetic resistances of circuit sections, where R_{pk} refer to poles, R_{gk} refer to air gaps between the poles and the rotor, R_{sk} refer to stator armature sections between two poles; R_{lk} are leakages between poles (air gaps) and R_{ak} are leakages in rotor sections; e_k are coil magnetomotive forces, where $e_1 = i_{c1}w_1, \ldots, e_8 = i_{c8}w_8$.
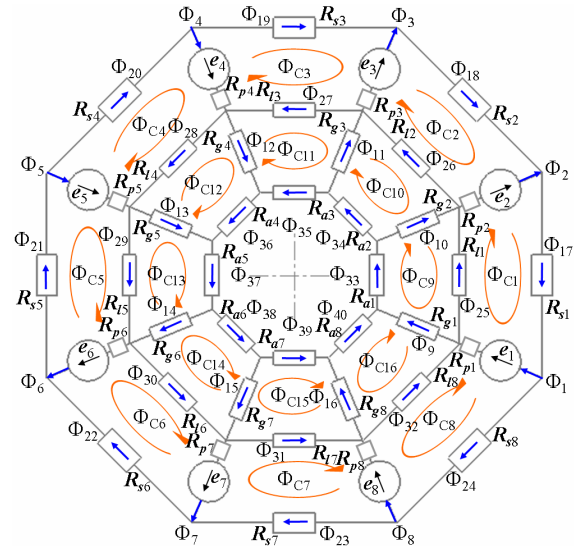

Figure 4. Equivalent electromagnetic circuit of AMB1.

The magnetic circuit of the radial AMB1 is calculated using a law identical to Kirchhoff's second law for electric circuits and an equivalent circuit

(Fig. 4). Magnetic circuits are calculated using different methods, including the node-potential or the loop flux ones. Using the loop flux method (an analog of the loop current method) yields a system of algebraic equations with respect to loop fluxes. Its solution allows finding loop fluxes used for determining the fluxes in all paths. Thus the fluxes in non-adjacent paths are equal to loop fluxes if their directions coincide, and are equal to loop fluxes with a reverse sign if they do not coincide. The fluxes in non-adjacent paths are also defined [Borisov, Lipatov, Zorin, 1985].

The magnetic fluxes Φ_{41} to Φ_{80} in the magnetic circuit of the radial AMB2 were determined using the same approach based on considering similar models and equivalent circuits (Figs. 2 and 4).

The magnetic circuit of the axial AMB3 were replaced with the schematic circuit, Fig. 5.

Fig. 5 has designations similar to those of magnetic fluxes, resistances and magnetomotive forces for AMB1 (Fig. 4).

The magnetic circuit of the axial AMB3 was calculated using this equivalent circuit and applying the loop flux or node-potential method.
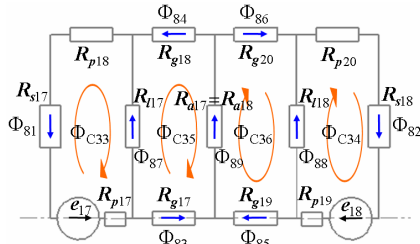

Figure 5. Equivalent circuit of the AMB3 electromagnetic circuit.

5.2 Determining magnetic resistances

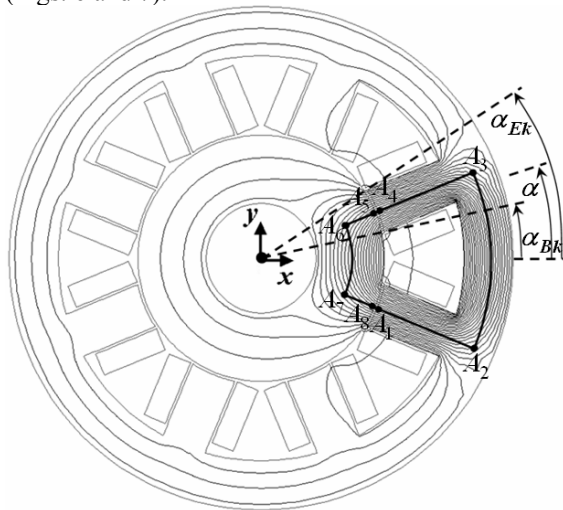The magnetic resistances of sections of AMB circuits are found using magnetic flux path diagrams (Figs. 6 and 7).

Figure 6. Schematic diagram of magnetic flux paths in AMB1.

Magnetic resistances R_{pk}, R_{sk}, R_{ak}, corresponding to sections A_1A_2, A_3A_4, A_2A_3 and A_5A_8, were found us-

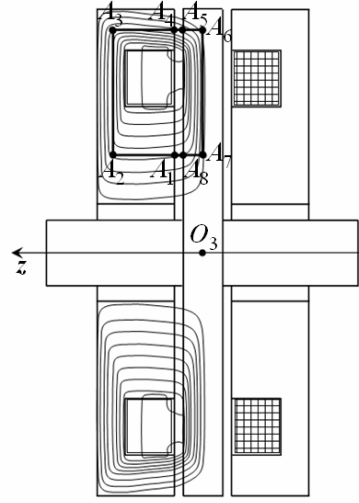ing (7) with account of the geometry of the sections and the characteristics of materials.

Figure 7. Schematic diagram of magnetic flux paths in AMB3.

Each leakage magnetic resistance R_{lk} for radial AMB was found approximately as a quantity inverse to conductance between two nonparallel surfaces. For the axial AMB, it was found using the technique of calculating a flat cylindrical lifting electromagnet based on the leakage flux path diagram [Roters, 1941].

All the above magnetic resistances depend only on the geometry of magnetic bearings and properties of materials.

At the same time, the magnetic resistances of air gaps R_{gk} also depend on the rotor current position. They are represented via magnetic conductances of gaps:

$$R_{gk} = \frac{1}{g_{gk}}, \qquad g_{gk} = \mu_0 \int_{S_k} \frac{dS}{h_k}, \qquad (10)$$

where g_{gk} is magnetic conductance of the gap under the k-th pole and h_k is height of the gap under the pole elementary area dS.

The gap magnetic conductance was determined with account of the mutual influence of rotor radial and axial displacements, and without account of this.

In the first case, the height h_k of the gap under dS depends on all mechanical generalised coordinates included in one group, for instance, $q=(x_1,y_1,x_2,y_2,z_3)$ [Martynenko, 2006], and in the second case, it depends only on some of them [Zhuravlyov, 2003].

Thus, simplified formulae for determining the height of the gap under the element area of the pole surface, which do not account for mutual influence of radial and axial displacements for AMB1, AMB2 and AMB3, have the form (11), (12) and (13), respectively:

$$h_k(x_1, y_1, \alpha) = \delta_{r1} - x_1 \cos\alpha - y_1 \sin\alpha , \quad (11)$$

$$h_k(x_2, y_2, \alpha) = \delta_{r2} - x_2 \cos\alpha - y_2 \sin\alpha , \quad (12)$$

$$h_k(z_3) = \delta_a \mp (z_3 + l_2 + l_3), \qquad (13)$$

where α is the angular coordinate measured from

axis O^*x, which changes within the angular coordinates of the beginning (α_{Bk}) and end (α_{Ek}) of the k-th pole of the radial AMB.

5.3 Calculation of magnetic conductances

Numerical experiments were conducted for the AMB-suspended rotor design shown in Fig. 1. It has the following parameters: l_1=0.105 m, l_2=0.101 m and δ_{r1}=δ_{r2}=δ_a=0.0005 m with an 0.023-m inner radius of the radial AMB stator. The conductances of air gaps under the pole of radial AMB1 (Figs. 8-9) and under the pole of axial AMB3 (Figs. 10-11) were determined. The solid lines in the plots show the conductances computed with the above first method, and the dotted lines show conductances computed using the second method.

The following situations were modelled:

1. Spatial rotation, i.e. simultaneous variation of x_1 from $-\delta_{r1}$ to δ_{r1} and x_2 from δ_{r2} to $-\delta_{r2}$ at $y_1=y_2=0$ (Fig. 8).

2. Rotation about the centre of gravity of the AMB1 journal, i.e. variation of x_2 from $-\delta_{r2}$ to δ_{r2} at $x_1=y_1=y_2=0$ (Fig. 9).

3. Axial displacement of the rotor turned about axis O^*x, i.e. variation of z_3 from 0 to δ_a at $x_1=x_2=y_2=0$ and $y_2=-\delta_{r1}$ (Fig. 10).

4. Rotation about the centre of gravity of the disk of the axial AMB3 within geometrically admissible limits (Fig. 11).
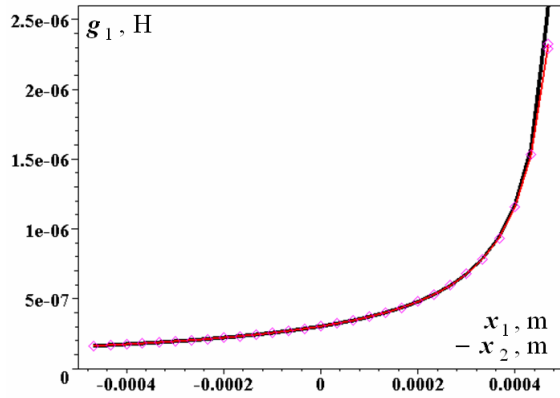

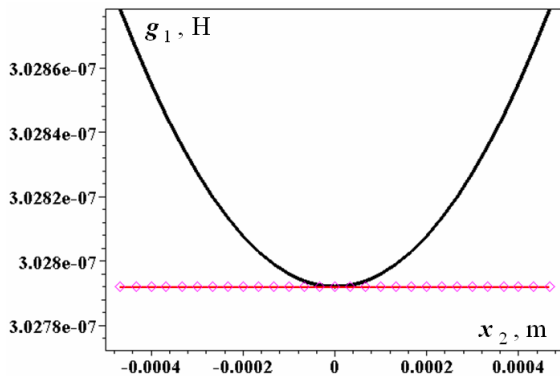Figure 8. Conductance of gap under pole 1 of AMB1 at spatial rotation.

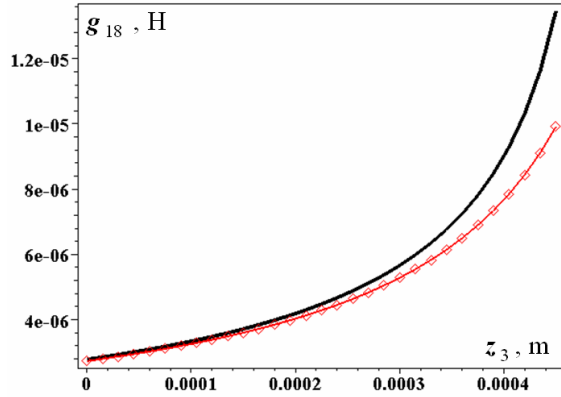Figure 9. Conductance of gap under pole 1 of AMB1 at rotation about journal centre of gravity.

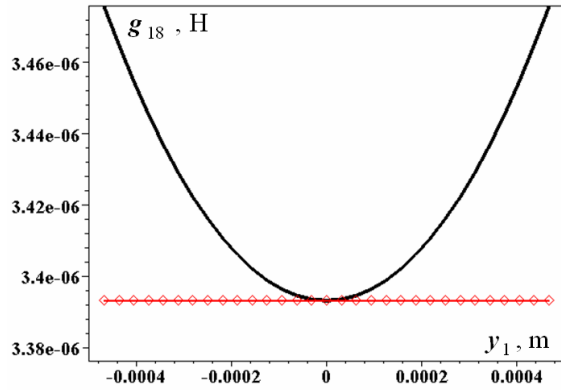Figure 10. Conductance of gap under pole 18 of AMB3 at rotor axial displacement.

Figure 11. Conductance of gap under pole 18 at rotation about the centre of gravity of the disk of the axial AMB3.

Analysis of results shows that close to the rotor central position ($\pm\delta/2$) the conductances obtained by the two above methods differ by less than 0.5 %, and are considered matching.

However, the error of computation of gap conductances with simplified expressions (11)-(13) when the actual gap tends to zero in some cases reaches 20 % (Figs. 8 and 10). This can result in inaccurate determination of magnetic resistances and fluxes, and hence, of magnetic field energy and suspension electromagnetic responses. Such an approach introduces an error into the mathematical model (3), which cannot be ignored in some cases. For instance, failing to account for this when defining or checking the parameters of the controller and the control algorithm with the help of numerical experiments can result in narrowing of the actual range of rotor motion stability within AMB gaps.

6 Numerical experiments

The considered nonlinear mathematical model of a suspension can serve as a basis of a simulation computer model (SCM) of a suspension for practical application in design research.

Fig. 12 shows an example of calculating the dynamic behaviour of the rotor with the help of such an SCM.

To obtain stable rotor motion in AMB, control voltages u_{ck} should vary definitely with time de-

pending on the complete state column-vector Z. For different control system options, Z can include different sets of measured variables. A feedback controller, which implements a specific control algorithm, changes the control voltages.
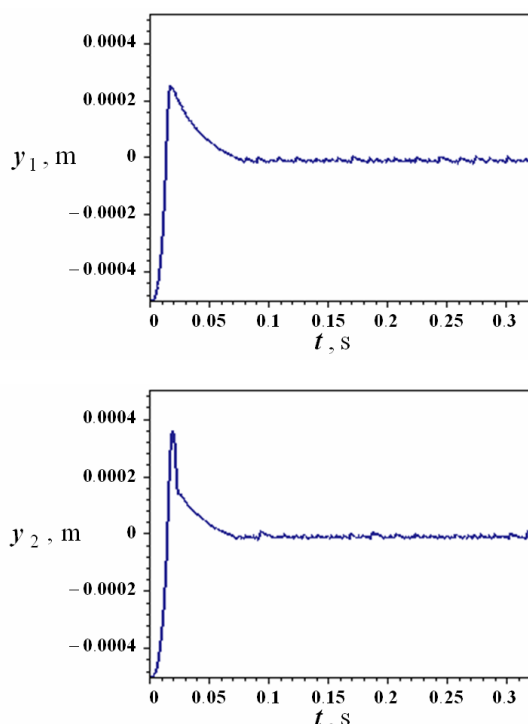

Figure 12. Vertical rotor displacement.

In this case, the possibility of controlling rotor motion with the algorithm [Rogovoj, Buholdin, Levashov, Martynenko, Smirnov, 2006] was investigated. According to this algorithm, the state column-vector Z includes all the mechanical generalised coordinates comprising one group, i.e. displacements, as well as the velocities and currents in electromagnet circuits.

The results of numerical experiments at the specified control mode simulate enabling of the control system with such initial conditions when all the parameters included in column-vector Z are equal to 0.

As analysis of results has shown (Fig. 12), maximum rotor displacements in transient conditions are roughly 75 % of the rated gap. This confirms the necessity of reserved usage of linearised mathematical models, which are always written down on the assumption of smallness of variable deviation from rated values.

7 Conclusion

The paper has considered the nonlinear mathematical model of a rigid rotor suspended in active magnetic bearings. The key feature of the simulation model constructed with the suggested mathematical model is the option of more adequate modelling of rotor-AMB behaviour when the rotor approaches the poles.

Models of such type can be used for numerical experiments in identifying the actual limits of using linear and nonlinear control algorithms and defining their parameters, which ensure stable rotor motion within the rated gap.

Another application of simulation computer models is developing and optimising rotor-AMB system control algorithms, as well as investigating the dynamic behaviour of this system with identification of resonance modes and subsequent offsetting from them.

References

Bessonov, L.A. (1973) *Theoretical Basics of Electrical Engineering*. Vysshaja Shkola, Moscow. (In Russian)

Borisov, Ju.M., Lipatov, D.N., Zorin, Ju.N. (1985) *Electrical Engineering*. Energoatomizdat, Moscow. (In Russian)

Hodzhaev, K.Sh. (1979) Vibrations of nonlinear electromechanical systems. *Vibrations in Engineering, Mashinostroenie, Moscow*, Vol. 2, pp. 331-347. (In Russian)

Martynenko, G.Yu. (2006) Correction of mathematical model of rotor on AMP due to determination of the magnetic conductivity of gaps under poles in view of mutual effect of displacements in radial and axial directions *Visnyk NTU "KhPI", Kharkiv, Ukraine*, Vol. 32, pp. 179-192. (In Russian)

Maslen, E.H. (2000) *Magnetic bearings*. University of Virginia Department of Mechanical, Aerospace, and Nuclear Engineering Charlottesville. Virginia.

Poznjak, Je.L. (1980) Vibrations of rotors. *Vibrations in engineering. Mashinostroenie, Moscow*, Vol. 3, pp. 130-187. (In Russian)

Rogovoj, E.D., Buholdin, Yu.S., Levashov, V.A., Martynenko, G.Yu., Smirnov, M.M. (2006) *Method of discrete control by electromagnetic suspension of rotating rotors*. Patent RU 2277190 C1, 10.07.2003. (In Russian)

Roters, H.C. (1941) *Electro-magnetic Devices*. John Wiley, USA.

Schweitzer G, Bleuler H, Traxler A. (1994) *Active Magnetic Bearings*. Hochschulverlag AG. Zurich.

Siegwart R, Bleuler H, Traxler A. (2000) *Industrial Magnetic Bearings*. Gordon and Breach Science Publisher, Amsterdam.

Steven M, Nataraj C. (2007) Suppression of Base Excitation of Rotors in Magnetic Bearings. *International Journal of Rotating Machinery*. Vol. 2007, Article ID 91276, 10 pages.

Zhuravlyov, Y.N. (2003) *Active magnetic bearings: Theory, calculation, application*. Polytekhnika. Saint Petersburg. (In Russian)